

energy of an assembly including fully formed  $H^+$  and  $HO^-$ . For other purposes, other choices of initial state might be appropriate. As one example, if the zero of energy had been taken as that of the assembly  $2H_2O + CH_2O$ , the reactions involving  $H^+$  or  $HO^-$  would have been displaced vertically upwards by an increment of 426 kcal/mol, with the result that the stepwise processes would no longer be energetically preferred over possible concerted processes.

**Factors Leading to Enforced Concertedness.** The properties of the stable cationic and anionic adducts,  $HOCH_2OH_2^+$  and  $HOCH_2O^-$ , give a clue to the major reason for the failure of water and formaldehyde to form a zwitterionic adduct **1** and the resulting enforced character of the concerted mechanism through **2**. Both of the ionic adducts have, as noted above, long, weak  $O\cdots C$  bonds to the nucleophile and short, strong  $C-O$  (former carbonyl) bonds. This suggests a tendency to permit sufficient attachment of the nucleophile and electrophile so that the charge on the ionic partner can be dispersed, but not sufficient bonding that the charge tends to become localized on a single atom (as in the simple valence-bond representations). Dissociation of the ionic adducts then requires work to sever the covalent attachments and reconcentrate the charge within the ionic partner.

Dissociation of the structure corresponding to **1**, in contrast, involves charge depolarization, and thus no energy barrier opposes its decomposition. Expressed differently, the formation of an adduct like **1** would necessarily relocate electron density, resulting in an excess of positive charge in the water fragment and an excess of negative charge in the formaldehyde fragment. The difficulty of achieving such a charge polarization is shown by the fact that when the "bond" to the nucleophilic oxygen is forced to 1.4 Å, the carbonyl group retains a  $C-O$  distance of 1.30 Å, substantially shorter than the corresponding distance in either the cationic or anionic adduct. These have equilibrium bond lengths to the nucleophile far longer than 1.4 Å. Adduct formation from neutral molecules must involve charge polarization, while formation of

"weak" adducts (with loose nucleophile attachment) in the ion-neutral reactions makes for charge dispersal. This presumably accounts for adduct stability and for the existence of feasible stepwise mechanisms in the ion-neutral reactions but an unbounded character of the "intermediate" and an enforced, concerted mechanism in the neutral-neutral reaction.

The transition state **2**, of course, also dissociates to water and formaldehyde with charge depolarization,<sup>52</sup> a process not resisted by an energy barrier. However, incipient bond formation between one of the hydrogens of the water fragment and the oxygen of the formaldehyde fragment opens another channel for decomposition with charge depolarization, namely, formation of methanediol. This process as well is attended by no opposing energy barrier. Thus **2**, with open, barrier-free pathways to both reactants and products, but bounded in other respects, is a transition state for the concerted reaction. The same physical factors account for the nonexistence of the intermediate **1** and for the fact that **2** exists as a transition state for the concerted reaction.

### Conclusions

These results provide models for enforced, concerted carbonyl addition and for stepwise, specific-acid-catalyzed and -base-catalyzed carbonyl addition in the gas phase. Their significance for carbonyl group reactions in more complex environments such as in aprotic solvents, in aqueous solution or in enzyme active sites, remains to be determined by further study. We are currently examining the properties of transition state **2** and the effect of introducing more water molecules into the system.

**Acknowledgment.** This work is supported in part by a grant from the National Institute of General Medical Sciences (R01-GM-20198).

(52) In fact, the atomic charge distributions for **2** and for a typical structure resembling **1** are very similar.<sup>49</sup>

## The Role of Nonadiabatic Coupling and Sudden Polarization in the Photoisomerization of Olefins

Maurizio Persico

Contribution from the Istituto di Chimica Fisica dell'Università di Pisa, I-56100 Pisa, Italy.  
Received April 7, 1980

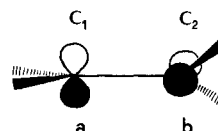
**Abstract:** Energies, dipoles, and nonadiabatic couplings have been computed for the diradicalic and zwitterionic states of ethylene and propene, in the  $3 \times 3$  CI approximation. The same kind of calculations, and qualitative arguments based on VB theory, are used to elucidate the nature of the perturbation of the zwitterionic states of an olefin, as caused by different kinds of substituents and/or by pyramidalization of a carbon atom adjacent to the double bond. The vibrational problem relative to the twisting coordinate is solved for propene and for ethylene at various pyramidalization angles. The properties of the vibronic states are determined both in the Born-Oppenheimer approximation and in a computational scheme which explicitly allows for nonadiabatic coupling. Finally, quantum mechanical calculations are performed to describe the time evolution of the molecular wave function after a Franck-Condon excitation. The paradigmatic value of the results here presented is discussed, mainly in relation to the open question of the existence of strong polar vibronic states in excited olefins, with a lifetime long enough to play a role in photochemical processes.

### Introduction

The problem of the photolysis of olefins has been variously and extensively dealt with by theoretical chemists in the past.

A large number of papers are concerned with the properties of the first electronic states of ethylene and other olefins (see ref 1-18 and references therein).

Chart I



At present the following points seem to be settled more or less definitively. (1) Three VB structures are most relevant to describe

(1) U. Kaldor and I. Shavitt, *J. Chem. Phys.*, **48**, 191 (1968).

the three lowest singlets of monoolefins at both planar and twisted geometries. Calling a and b the p (localized) orbitals of Chart I, we shall have a covalent-diradical structure  $(2 + 2S_{ab}^2)^{-1/2}(ab + ba)$  and two ionic structures  $a^2$  and  $b^2$ ; their mixing corresponds to performing a  $3 \times 3$  configuration interaction with two electrons in two orbitals,  $\psi_+ = (2 + 2S_{ab})^{-1/2}(a + b)$  and  $\psi_- = (2 - 2S_{ab})^{-1/2}(a - b)$ .<sup>19</sup> In the nonpyramidalized ethylene the ground state (D) is prevalently covalent at the planar geometry and is a pure diradical at the twisted one. The excited singlets  $Z_1$  and  $Z_2$  are ionic in character; their energy has a minimum at the twisted geometry (twisting angle  $\theta = 90^\circ$ ). The rigid excitation of planar ethylene to  $Z_1$  (the V state in Mulliken's notation) is actually a mixed valence-Rydberg transition, but the Rydberg character disappears when twisting.<sup>3,7,13-15</sup> (2) At planar geometries the ionic structures  $a^2$  and  $b^2$  are strongly mixed. At  $\theta = 90^\circ$ , however, their interaction matrix element,  $K_{ab}$ , becomes very small; thus, if any dissymmetry removes the degeneracy of the orbitals a and b,  $Z_1$  and  $Z_2$  become nearly pure  $a^2$  and  $b^2$  states with large dipole moments.<sup>4,5</sup> When  $\theta$  departs from the value of  $90^\circ$ , the increase of  $K_{ab}$  cancels more or less rapidly the polarization. In the *s-cis*, *s-trans* diallyl a strong dipole is found in the range of only  $2-4^\circ$  around  $\theta = 90^\circ$ ;<sup>5,10,12</sup> here the dissymmetry is given by the difference between stereoisomeric substituents.

The only other molecule studied under this point of view is ethylene, pyramidalized at one end;<sup>5,9,16-18</sup> in this case the polarization extends over a much wider range, some tens of degrees.<sup>18</sup> The name which currently designates the phenomenon, "sudden polarization", witnesses the large influence of the calculations on the *s-cis*, *s-trans* diallyl on the theoretical ideas about the problem; by the way, it is worth noting that, until very recently, the only reported curve of the dipole moment vs. the twisting angle  $\theta$  was that of ref 5.

The sudden polarization has been invoked to account for the stereospecificity observed in the photocyclization of certain conjugated polyenes, to explain the action of the visual chromophore, etc. (ref 20 and 21 and references therein).

Apart from the electronic problem, there are other aspects of the question which have been dealt with less extensively in the past.

First of all, it has been shown that the transition to  $Z_1$  is essentially nonvertical; indeed its interpretation requires that at

least one vibrational motion should be considered, the twisting around the double bond.<sup>22,23</sup>

Consideration of the nonadiabatic coupling came later. Orlandi et al. set up a model of the ionic states  $Z_1$  and  $Z_2$ , yielding reasonable analytic expressions for the charge displacement along the C-C axis,  $\Delta q(\theta)$ , and for the nonadiabatic coupling matrix element  $\langle Z_1 | \partial / \partial \theta | Z_2 \rangle$ .<sup>24</sup> The model parameters were fitted on the ab initio calculations for the *s-cis*, *s-trans* diallyl<sup>5</sup> with some extra variability left to show the effect of more dissymmetric substituents. The charge separation  $\Delta q(\theta)$  was averaged in the lowest vibrational states of  $Z_1$  and  $Z_2$ ; due to the narrowness of the peak of the  $\Delta q(\theta)$  function, its computed average was about 5-30 times smaller than the maximum value at  $\theta = 90^\circ$ . The matrix element of the nonadiabatic coupling operator between the same vibronic states was also small, with respect to the energy separation.

Weiss and Warshel, finally, computed the nonadiabatic coupling (twisting coordinate) in both ethylene and retinal, from electronic wave functions obtained by semiempirical methods.<sup>25</sup> They found that  $\langle D | \partial / \partial \theta | Z_1 \rangle$ , as a function of  $\theta$ , has a large and narrow peak around  $\theta = 90^\circ$ , nearly a  $\delta$  function. A simple semiclassical argument shows that, in this case, the  $Z_1$ -D transition probability is nearly 1 already during the first twisting oscillation of the molecule in the excited state. This is a possible way to explain the high quantum yields (>0.5) observed in the *cis-trans* photoisomerization of cyclooctene and stilbene.

Both the works of Orlandi et al. and Weiss et al. end up by denying, for different reasons, the existence, during a reasonably long time at the molecular scale, of vibronic states exhibiting a large charge separation, i.e., essentially, the sudden polarization effect and all the speculations based on it.

The present investigation aims at giving a unified treatment of (a) the charge separations caused both by pyramidalization and by substitution, (b) the nonadiabatic coupling between the D,  $Z_1$ , and  $Z_2$  states, and (c) the quantum dynamical time evolution of a molecule after excitation to  $Z_1$  (or  $Z_2$ ), including nonadiabatic transition to D and  $Z_2$  (or  $Z_1$ ) while oscillating along the twisting coordinate.

### Electronic States of Ethylene

All the electronic calculations here reported have been performed at a modest ab initio level, making use of the "half-electron" effective Hamiltonian in the SCF procedure,<sup>26</sup> followed by a  $3 \times 3$  CI for the configurations  $\psi_+^2$ ,  $\psi_+\psi_-$ , and  $\psi_-^2$ ; the atomic basis set was the STO-3G minimal basis of Pople and co-workers; all the calculations were performed with the GUASSIAN 70 program.<sup>27</sup> The main advantage of the method consists of a balanced utilization of the a and b orbitals, which is not warranted by the usual closed-shell SCF procedure.<sup>9</sup> The drawbacks, mainly due to the very limited CI, are also well-known:<sup>8</sup> not allowing for the  $\sigma$ -electron polarization in the zwitterionic states, opposite to that of the  $\pi$  electrons, one overestimates the total dipole moment; other effects which can be allowed for only by large CI's concern the conjugated polyenes. Of course the minimal basis cannot represent the partial Rydberg character of the planar  $Z_1$  state, but, as we are chiefly interested in the region around  $90^\circ$  of twisting, this is not too serious a disadvantage.

Altogether, our calculations grossly reproduce the qualitative features encountered in the best CI treatments<sup>16-18</sup> concerning potential energy curves,  $Z_1 - Z_2$  energy separations, variation of the dipole moment with the twisting and pyramidalization, etc.; hence one can be confident also on the computed nonadiabatic couplings  $g_{12} = \langle D | \partial / \partial \theta | Z_1 \rangle$ ,  $g_{13} = \langle D | \partial / \partial \theta | Z_2 \rangle$ , and  $g_{23} =$

(2) T. H. Dunning, Jr., W. J. Hunt, and W. A. Goddard III, *Chem. Phys. Lett.*, **4**, 167 (1969).

(3) H. Basch and V. Mc Koy, *J. Chem. Phys.*, **53**, 1628 (1970).

(4) C. E. Wulfman and S. Kumei, *Science (Washington, D. C.)*, **172**, 1061 (1971).

(5) V. Bonačić-Koutecký, P. Bruckmann, P. Hiberty, J. Koutecký, Koutecký, Leforestier, and L. Salem, *Angew. Chem., Int. Ed. Engl.*, **14**, 575 (1975).

(6) P. Bruckmann and L. Salem, *J. Am. Chem. Soc.*, **98**, 5037 (1976).

(7) L. E. Mc Murchie and E. R. Davidson, *J. Chem. Phys.*, **66**, 2959 (1977).

(8) M. C. Bruni, J. P. Daudey, J. Langlet, J.-P. Malrieu, and F. Momicholi, *J. Am. Chem. Soc.*, **99**, 3587 (1977).

(9) G. Berthier, B. Lévy, and L. Praud, *Gazz. Chim. Ital.*, **108**, 377 (1978).

(10) V. Bonačić-Koutecký, J. Cizek, D. Döhnert, and J. Koutecký, *J. Chem. Phys.*, **69**, 1168 (1978).

(11) V. Bonačić-Koutecký, *J. Am. Chem. Soc.*, **100**, 396 (1978).

(12) C. M. Meerman van Benthem, H. J. C. Jacobs, and J. J. C. Mulder, *Nouv. J. Chim.*, **2**, 123 (1978).

(13) S. D. Peyerimhoff, *Gazz. Chim. Ital.*, **108**, 411 (1978).

(14) R. J. Buenker, S. D. Peyerimhoff, and S. Shih, *J. Chem. Phys.*, **69**, 3882 (1978).

(15) R. J. Buenker, S. D. Peyerimhoff, and S. Shih, *Chem. Phys.*, **36**, 97 (1979).

(16) B. R. Brooks and H. F. Schaefer III, *J. Am. Chem. Soc.*, **101**, 307 (1979).

(17) V. Bonacic-Koutecký, R. J. Buenker, and S. D. Peyerimhoff, *J. Am. Chem. Soc.*, **101**, 5917 (1979).

(18) V. Bonacic-Koutecký, R. J. Buenker, and L. Pogliani, to be submitted for publication.

(19) L. Salem and C. Rowland, *Angew. Chem., Int. Ed. Engl.*, **11**, 92 (1972).

(20) L. Salem in "Excited States in Organic Chemistry and Biochemistry", B. Pullmann and N. Goldblum, Eds., 1977, p 163.

(21) L. Salem, *Acc. Chem. Res.*, **12**, 87 (1979).

(22) S. D. Peyerimhoff and R. J. Buenker, *Theor. Chim. Acta*, **27**, 243 (1972).

(23) A. Warshel and M. Karplus, *Chem. Phys. Lett.*, **17**, 7 (1972).

(24) G. Orlandi, P. Palmieri, and G. Poggi, *Chem. Phys. Lett.*, **68**, 251 (1979).

(25) R. M. Weiss and A. Warshel, *J. Am. Chem. Soc.*, **101**, 6131 (1979).

(26) N. C. Baird and R. F. Barr, *Theor. Chim. Acta*, **36**, 125 (1974).

(27) W. J. Hehre, W. A. Lathan, R. D. Ditchfield, M. D. Newton, and J. A. Pople, QCPE Program No. 236.

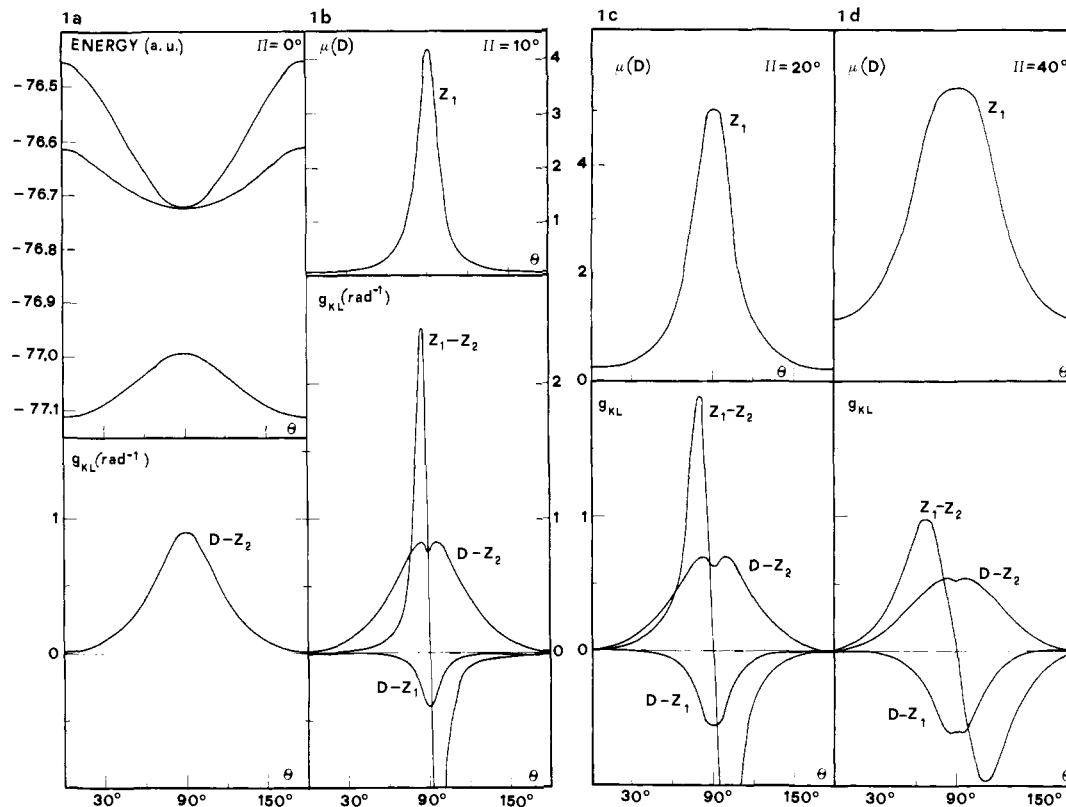


**Figure 1.** (a) Upper part: potential energy curves,  $U_K(\theta)$ . Lower part: nonadiabatic coupling function,  $g_{13}(\theta)$ , for nonpyramidalized ethylene ( $\pi_1 = \pi_2 = 0^\circ$ ). (b) Upper part: dipole moment along the C-C axis in the  $Z_1$  state,  $\mu_2(\theta)$ . Lower part: nonadiabatic coupling functions  $g_{KL}(\theta)$ , with  $\pi_1 = 10^\circ$  and  $\pi_2 = 0^\circ$ . (c) As in part b, with  $\pi_1 = 20^\circ$ ; (d) As in part b, with  $\pi_1 = 40^\circ$ .

**Table I.** Symmetry Representations of the Electronic States and Operators of Interest in Ethylene

	$\pi_1 = \pi_2 = 0^\circ$ $\theta = 0^\circ$	$\pi_1 = \pi_2 = 0^\circ$ intermediate $\theta$	$\pi_1 = \pi_2 = 0^\circ$ $\theta = 90^\circ$	$\pi_1 \neq 0^\circ$ , $\pi_2 = 0^\circ$ $\theta = 0^\circ$	$\pi_1 \neq 0^\circ$ , $\pi_2 = 0^\circ$ $\theta = 90^\circ$
point group	$D_{2h}$	$D_2$	$D_{2d}$	$C_s$	$C_s$
D state	$A_{1g}$	$A_1$	$B_1$	$A'$	$A''$
$Z_1$ state	$B_{1u}$	$B_1$	$B_2$	$A'$	$A'$
$Z_2$ state	$A_{1g}$	$A_1$	$A_1$	$A'$	$A'$
$\theta$ coord, $\partial/\partial\theta$ operator	$A_{1u}$	$A_1$	$B_1$	$A''$	$A''$
$\pi$ coord, $\partial/\partial\pi$ operator	$B_{2u}, B_{3g}^a$	$B_2, B_3^a$	$E^b$	$A'^c$	$A'^c$
$\hat{\mu}_Z$ operator	$B_{1u}$	$B_1$	$B_2$	$A'$	$A'$

<sup>a</sup> Simultaneous pyramidalization of both ends, either in phase or out of phase. <sup>b</sup> Degenerate, independent pyramidalizations of either end (as in Figure 2). <sup>c</sup> Variation of  $\pi_1$ , pyramidalization of the carbon atom  $C_1$ .

$\langle Z_1 | \partial/\partial\theta | Z_2 \rangle$  and other features not previously reported (we shall hereafter use the indices 1, 2, and 3 instead of D,  $Z_1$ , and  $Z_2$  in labeling the matrix elements such as  $g_{12}$  etc.).

The  $g_{KL}$  couplings have been numerically computed with a technique described elsewhere, which could be called "finite differences of electronic wave functions."<sup>28-30</sup> It requires the determination of the wave functions at two different values of the nuclear coordinate,  $\theta$  and  $\theta + \Delta$ , at least. Actually, in this work we have adopted a 3-point procedure ( $\theta$  and  $\theta \pm \Delta$ ), which warrants a higher accuracy, with  $\Delta = 0.02^\circ$ ; at  $\theta = 90^\circ$ , where the choice of  $\Delta$  turns out to be critical, a 7-point formula ( $\theta, \theta \pm \Delta, \theta \pm 2\Delta, \theta \pm 3\Delta$ ) yields a substantial improvement.

The definition of the  $\partial/\partial\theta$  operator is such that both  $-CH_2$  groups rotate in opposite directions (by  $\Delta/2$  in the numerical procedure), about the C-C axis. If one should change this definition, for example, by holding one end fixed, the resulting matrix elements would be slightly different (ref 30 and references therein; see also a preliminary report on this work<sup>31</sup>).

In the calculations on ethylene the following geometrical parameters were adopted:  $R_{CC} = 1.400 \text{ \AA}$ ,  $R_{CH} = 1.076 \text{ \AA}$ ,  $\angle HCH = 116.6^\circ$ .<sup>16</sup> The pyramidalization angle of  $C_1$ ,  $\pi_1$ , is fixed successively at  $0^\circ$  ( $H_2C-C$  atoms on the same plane),  $10^\circ$ ,  $20^\circ$ , and  $40^\circ$ ; for each value of  $\pi_1$ , the calculation is repeated at  $\theta = 0, 20, 40, 50, 60, 65, 70, 75, 80, 85, \text{ and } 90^\circ$ .

Parts a-d of Figure 1 show the most interesting quantities which are functions of  $\theta$ , at four fixed values of  $\pi_1$  ( $\pi_2 = 0^\circ$ ): the nonadiabatic coupling matrix elements,  $g_{KL}$ , and the dipole moment  $\mu_{22}$  along the C-C axis in the  $Z_2$  state (the perpendicular components, much smaller, will be consistently neglected). For  $\pi_1 = \pi_2 = 0^\circ$  ( $D_2$  symmetry), the dipole vanishes identically (see Table I), and, instead of  $\mu_{22}$  we report the potential energy curves  $U_1, U_2$ , and  $U_3$ , which are qualitatively similar at all pyramidalization angles.

The molecular symmetry group, as defined by Longuet-Higgins,<sup>32</sup> for twisting ethylene at a fixed  $\pi_1$  ( $\pi_2 = 0^\circ$ ) is isomorphic to  $C_{2v}$ ; we shall thus label the functions of  $\theta$   $A_1, A_2, B_1$ , and  $B_2$ , following their parity with respect to  $\theta = 0$  and  $180^\circ$  and to  $\theta = 90^\circ$  and  $270^\circ$ ; we state by convention:  $A_1 \equiv (\text{even}, \text{even})$ ,  $A_2 \equiv (\text{odd}, \text{odd})$ ,  $B_1 \equiv (\text{even}, \text{odd})$ ,  $B_2 \equiv (\text{odd}, \text{even})$ . Simple consid-

(28) C. Galloy and J. C. Lorquet, *J. Chem. Phys.* **67**, 4672 (1977).

(29) G. Hirsch, P. J. Bruna, R. J. Buenker, and S. D. Peyerimhoff, *Chem. Phys.* **45**, 335 (1980).

(30) R. Cimraglia, M. Persico, and J. Tomasi, to be submitted for publication.

(31) M. Persico, Rapport d'Activité Scientifique du CECAM, 1979.

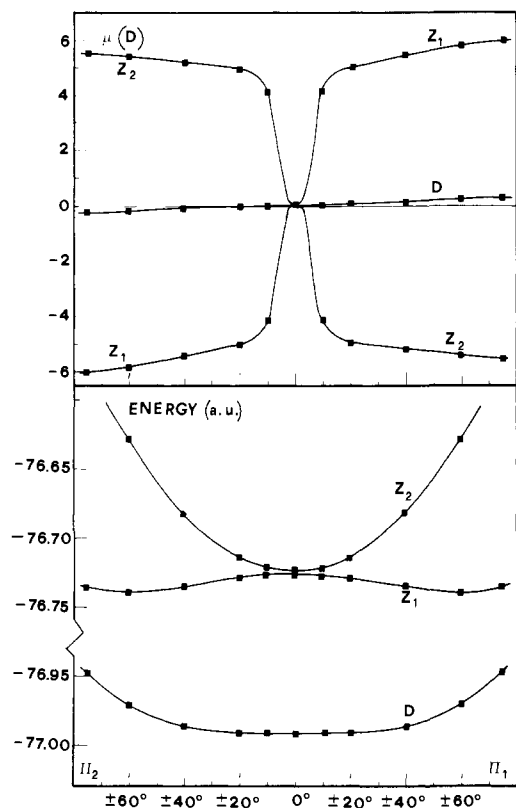


**Figure 2.** Upper part: dipole moments,  $\mu_k$ . Lower part: potential energy curves  $U_k$ , for twisted ethylene ( $\theta = 90^\circ$ ), as functions of the pyramidalization angle. On the right-hand side,  $\pi_2 = 0^\circ$  and  $\pi_1$  is variable and vice versa on the left-hand side.

erations on the basis of Table I lead to the following assignments: all the diagonal matrix elements and  $\mu_{23}$  belong to the  $A_1$  irreducible representation;  $g_{23}$  to  $A_2$ ;  $\mu_{12}$  and  $\mu_{13}$  to  $B_1$ ;  $g_{12}$  and  $g_{13}$  to  $B_2$ . Moreover,  $\mu_{kk}$ ,  $\mu_{13}$ ,  $g_{12}$ , and  $g_{23}$  vanish for  $\pi_1 = \pi_2 = 0^\circ$ .

Besides these formal constraints, we shall try to discuss the trends shown in Figures 1 and 2 on physical grounds.

The origin of the opposite dipole moments  $\mu_{22}$  and  $\mu_{33}$  has been already widely discussed elsewhere.<sup>4,5,10,20,21,24</sup> At  $\theta = 90^\circ$ , their increase is dramatic going from  $\pi = 0^\circ$  to  $\pi = 20^\circ$  and much slower afterwards. This happens because it is very easy to induce a demixing of the  $a^2$  and  $b^2$  ionic structures, whose interaction matrix element,  $K_{ab}$ , is only 0.7–0.8 kcal/mol; the change in hybridization, from  $sp^2$  toward  $sp^3$ , then induces an abrupt change in the electronic wave functions, by lowering the energy of the  $a$  orbital. On the contrary, the width of the peak in  $\mu_{22}$  and  $\mu_{33}$  increases steadily with  $\pi$ , as the balance between  $K_{ab}$  at intermediate values of  $\theta$ , and the energy difference  $\Delta E = E(b^2) - E(a^2)$  ( $>0$ ) is gradually displaced in favor of  $\Delta E$ . The shape of the energy curves of the ionic states along the  $\theta$  coordinate is strongly dependent on  $\pi$ . For twisted ethylene, the demixing of  $a^2$  and  $b^2$  is accompanied by a stabilization of  $Z_1$  and a much larger destabilization of  $Z_2$ . Starting from the planar geometry the converse occurs; i.e.,  $Z_2$  is stabilized by the pyramidalization; here the major role is probably played by the  $K_{ab}$  integral, whose effect is to split the energies of  $Z_1$  ( $a^2 - b^2$ ) and  $Z_2$  ( $a^2 + b^2$ ) and whose value is decreased in going from  $sp^2$  to  $sp^3$ .

The dipole moment in the ground state, of covalent-diradicalic character, is small everywhere. For a given  $\pi$ , it is larger at  $\theta = 0^\circ$ , where some admixing of ionic character is present, than at  $\theta = 90^\circ$ .

The variation of the transition dipoles with the twisting angle has been paid less attention in the past.<sup>22</sup> The largest transition moment arises between the combination of VB structures<sup>33</sup>  $2^{-1/2}(a^2$

+  $b^2$ ) and  $2^{-1/2}(a^2 - b^2)$  and is of the order of  $R_{CC}$ , in au. Thus  $\mu_{23}$  is large (5–6 D) both at  $\theta = 0$  and  $180^\circ$  (variable  $\pi$ ) and at  $\pi_1 = 0^\circ$  (all  $\theta$ 's), but it drops to less than 1 D in twisted and pyramidalized ethylene (what is gained in polarity, in the zwitterionic states, is lost in polarizability). The transition dipole  $1/2\langle ab + ba | z | a^2 - b^2 \rangle$  is smaller and roughly proportional to  $S_{ab}$  so that  $\mu_{12}$  decreases harmonically when twisting from  $\theta = 0^\circ$  to  $\theta = 90^\circ$ .  $\langle ab + ba | z | a^2 + b^2 \rangle$  vanishes in the  $D_2$  symmetry, and consequently  $\mu_{13}$  is small everywhere.

The simplified model of Orlandi et al.<sup>24</sup> accounts fairly well for the computed features of the  $g_{23}$  coupling function. In practice, they write the zwitterionic wave functions as  $|Z_1\rangle = (\cos \varphi)|a^2\rangle - (\sin \varphi)|b^2\rangle$  and  $|Z_2\rangle = (\sin \varphi)|a^2\rangle + (\cos \varphi)|b^2\rangle$  (zero  $S_{ab}$  overlap approximation); the small admixing of diradicalic character is ignored. Also, they neglect the  $\langle a^2 | \partial/\partial\theta | b^2 \rangle$  matrix element, to get  $g_{23} = \partial\varphi/\partial\theta$ . The parameter  $\varphi = \varphi(\pi_1, \theta)$  is close to  $\pi/4$  for  $\theta = 0^\circ$  and approaches  $\pi$  for  $\theta = 90^\circ$ ; its change is concentrated near the end of this range of values of  $\theta$ , where  $g_{23}$  has a maximum. For the reasons discussed above, the maximum in  $g_{23}$  is higher and narrower at smaller pyramidalization angles (see Figure 1b–d).

The origin of the  $g_{12}$  and  $g_{13}$  nonadiabatic couplings is less evident; in the VB language, one would thoroughly take into account the nonorthonormality of  $2^{-1/2}(ab + ba)$ ,  $a^2$ , and  $b^2$ , which makes the three-state treatment very tedious; the delocalized MO picture is here totally inadequate: suffice it to say that, around  $\theta = 90^\circ$ , the MO-SCF coefficients and the CI vectors undergo a very rapid variation, without any correspondence in the physical nature of the wave functions nor in the weights of the VB structures. We shall try to bring out the main contributions to the nonadiabatic coupling, without giving here a thorough treatment. (a) Let us start from the simplified situation where  $\pi_1 = \pi_2 = 0^\circ$ , so that  $g_{12}$  vanishes. The D and  $Z_2$  states result from a nonunitary transformation in the subspace spanned by  $2^{-1/2}(ab + ba)$  and  $2^{-1/2}(a^2 + b^2)$ ; however, a mixing parameter  $\alpha(\theta)$  can always be defined, in analogy to what has previously been done for  $Z_1$  and  $Z_2$  in the pyramidalized conformations, then,  $g_{13}$  will contain a term such as  $\partial\alpha/\partial\theta$ . The parameter  $\alpha$ , which represents the admixing of ionic character in the D state, will go from its largest absolute value, at  $\theta = 0$  and  $180^\circ$ , to zero, at  $\theta = 90^\circ$ , with  $\alpha(0^\circ) = -\alpha(180^\circ)$  (this change of sign is connected to the crossing of the  $\psi_+^{2-}$  and  $\psi_-^{2-}$  configurations<sup>19</sup>). The maximum value of its derivative should be found at  $\theta = 90^\circ$ ; indeed, from our calculations, it turns out that this is the main contribution to the nonadiabatic coupling ( $\sim 80\%$  of the total at  $\theta = 90^\circ$ ). As the pyramidalization mixes  $Z_1$  and  $Z_2$ , the maximum of  $\langle D | \partial/\partial\theta | Z_2 \rangle$  becomes less pronounced, and the coupling with the D state is shared also by  $Z_1$ . (b) A smaller, but not negligible, contribution comes from matrix elements such as  $\langle ab + ba | \partial/\partial\theta | b^2 \rangle = \langle a | \partial/\partial\theta | b \rangle$ ; it is directly related to the rotation of the localized orbital  $b$  with respect to  $a$ . If we regard  $a$  and  $b$  as pure p orbitals, we can write  $\langle a | b \rangle = S_{ab} = s \cos \theta$ , where  $s = S_{ab}$  at  $\theta = 0^\circ$  and  $\langle a | \partial/\partial\theta | b \rangle = -s/2 \sin \theta$ . Now, in planar ethylene  $s \approx 0.2$ , and it will be even smaller in the pyramidalized geometry, so that this contribution is less important than  $\partial\alpha/\partial\theta$ . We note in passing that the existence of a nonvanishing matrix element  $\langle a | \partial/\partial\theta | b \rangle$  prevents us from considering the VB structures as (approximate) diabatic states (see ref 34 and references  $\langle a | \partial/\partial\theta | b \rangle$ ) (c) Last, let us recall that in pyramidalized ethylene the most dramatic changes in the zwitterionic states occur near  $\theta = 90^\circ$ ; the rate of variation of, say,  $Z_2$ , in the scheme of Orlandi et al., can be written as  $\partial\varphi/\partial\theta | \partial Z_2 / \partial\varphi \rangle = \partial\varphi/\partial\theta [(\cos \varphi)|a^2\rangle - (\sin \varphi)|b^2\rangle]$ . This function has a small overlap with the  $(2 + 2S_{ab}^2)^{-1/2}(ab + ba)$  VB structure which dominates in the D state

$$\frac{\partial\varphi}{\partial\theta} \left\langle D \left| \frac{\partial Z_2}{\partial\varphi} \right. \right\rangle \approx \frac{\partial\varphi}{\partial\theta} \frac{\sqrt{2}S_{ab}}{\sqrt{1 + S_{ab}^2}} (\cos \varphi - \sin \varphi)$$

This third contribution is responsible for the small humps in the graphs of  $g_{12}$  and  $g_{13}$ , arising where  $\partial\varphi/\partial\theta$  is larger (see Figure 1b–d but not Figure 1a).

(32) H. C. Longuet-Higgins, *Mol. Phys.*, **6**, 445 (1963).

(33) Hereafter, for the sake of simplicity, we shall adopt the zero overlap approximation, whenever a more rigorous treatment is not strictly required; so we shall write  $2^{-1/2}(ab + ba)$  instead of  $(2 + 2S_{ab}^2)^{-1/2}(ab + ba)$  etc.

(34) R. Cimiraglia and M. Persico, *Mol. Phys.*, **38**, 1707 (1979).

Chart II

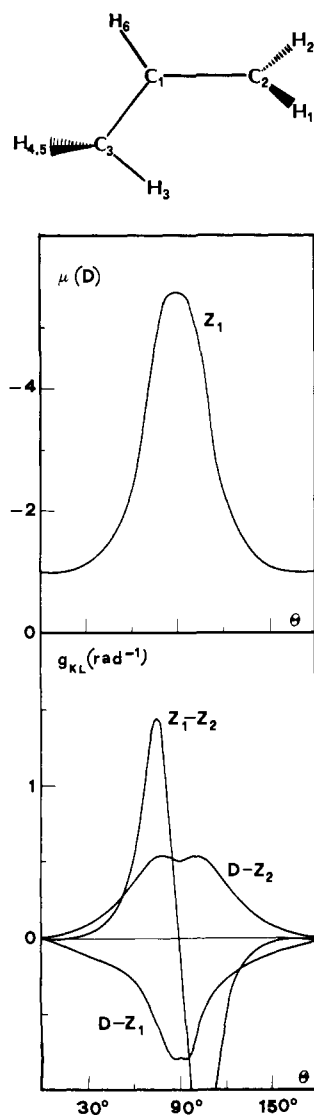


Figure 3. Dipole moment along the C-C axis in the  $Z_1$  state and nonadiabatic coupling functions, for nonpyramidalized propene.

Altogether, our computed  $g_{12}(\theta)$  curve appears to be very different from that computed by Weiss and Warshel,<sup>25</sup> so sharply peaked around  $\theta = 90^\circ$ ; of course, this is important as to the effectiveness of the nonadiabatic coupling (see below). It seems that the semiempirical wave functions of ref 25 lead to overestimating the ionic character of the D state (with a charge separation of about 0.4 electronic charges) and consequently the contribution  $a$  to  $g_{12}$ ; another source of variance is probably the angle step  $\Delta = 1^\circ$ , employed in ref 25 to make the numerical derivative, which is too large.<sup>35</sup>

#### Propene and Other Substituted Ethylenes

In order to compare the effect of the pyramidalization with that of substitution, we have performed a series of calculations on propene, with the experimental geometry of ref 36; some minor adaptations concern the twisting  $-\text{CH}_2$  end:  $R(\text{C}_1-\text{C}_2) = 1.400 \text{ \AA}$  (as in ethylene),  $R(\text{C}_2-\text{H}) = 1.086 \text{ \AA}$ ,  $\angle\text{C}_1\text{C}_2\text{H} = 121^\circ$  (see Chart II). The twisting angle,  $\theta$ , runs on the same set of values as in ethylene. Here the  $\partial/\partial\theta$  operator is defined so that only the lighter subfragment rotates (the  $-\text{CH}_2$  group). The results are shown in Figure 3.

At twisted geometries, in the  $Z_1$  state, the dipole is about  $-5.5 \text{ D}$ , opposite to that of ethylene pyramidalized in  $\text{C}_1$ . The dipole

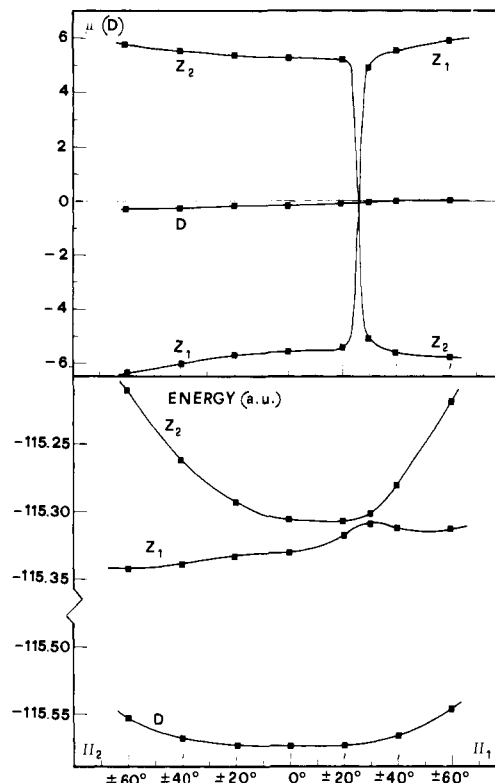


Figure 4. Dipole moment and potential energy curves for twisted propene, as in figure 2.

itself is not a good measure of the strength of the perturbation caused by the unsymmetrical substitution. For the reasons discussed in the preceding section, it is preferable to look at more meaningful quantities, namely: (a) the  $Z_1 - Z_2$  minimum energy separation,  $0.026 \text{ au}$ ; (b) the width of the polarization band around  $\theta = 90^\circ$ , about  $50^\circ$ ; (c) the maximum of the coupling function  $\langle Z_1 | \partial/\partial\theta | Z_2 \rangle$ ,  $1.44 \text{ rad}^{-1}$  at  $\theta = 75-80^\circ$ . All these indicators place the unpyramidalized propene between the ethylene with  $\pi_2 = 20^\circ$  and that with  $\pi_2 = 40^\circ$ .

A more direct comparison is carried out by pyramidalizing the propene itself at  $\theta = 90^\circ$ ; of course, here the behavior with respect to the pyramidalization of either  $\text{C}_1$  or  $\text{C}_2$  is in no way symmetrical (compare Figures 2 and 4). The  $\text{C}_2$  pyramidalization ( $\pi_2 \neq 0$ ), which favors the  $b^2$  configuration, leads to a stabilization of  $Z_1$  with a slight increase in the dipole moments. On the contrary, for  $\pi_1 \neq 0$  the  $Z_1$  energy rises, and the dipoles diminish, up to  $\pi_1 \approx 30^\circ$ , where the opposite effects of pyramidalization and substitution are balanced; here the  $Z_1 - Z_2$  energy separation is merely due to the small  $K_{ab}$  integral; for  $\pi_1 > 30^\circ$ , we find again a shallow minimum in  $Z_1$ , with reversed dipoles.

The perturbative effect of the  $-\text{CH}_3$  group in twisted propene can be explained with the same kind of arguments already applied by Hoffmann et al. to the  $\text{CH}_3-\text{CH}_2$  anions and cations.<sup>37</sup> The  $-\text{CH}_3$  group bears two orbitals which can interact with the a orbital of  $\text{C}_1$ ; they are essentially linear combinations of a  $2p$  orbital on  $\text{C}_3$  with the  $1s$  orbitals on  $\text{H}_4$  and  $\text{H}_5$  and will be called  $c$  (bonding, doubly occupied) and  $c^*$  (antibonding, vacant). Now, let us examine the energy of the  $a^2$  ionic structure: the  $a-c$  interaction, between two occupied orbitals, has a destabilization effect; the comparable  $a-c^*$  interaction (occupied-vacant) is stabilizing. The  $b^2$  structure is stabilized by  $a-c$  and unaffected by  $a-c^*$ , hence it is lower in energy than  $a^2$ . This conclusion is in agreement with the computed orientation of the dipole moment.

One could now ask what would happen when the  $-\text{CH}_3$  group is substituted by, say, a halogen atom. In this case the  $c^*$  orbital is absent,  $a^2$  is merely destabilized by the  $a-c$  interaction, and  $b^2$

(35) A. Warshel, private communication.

(36) D. R. Lide, Jr., and D. Christensen, *J. Chem. Phys.*, **35**, 1374 (1961).

(37) R. Hoffmann, L. Radom, J. A. Pople, P. von R. Schleyer, W. J. Hehre, and L. Salem, *J. Am. Chem. Soc.*, **94**, 6221 (1972).

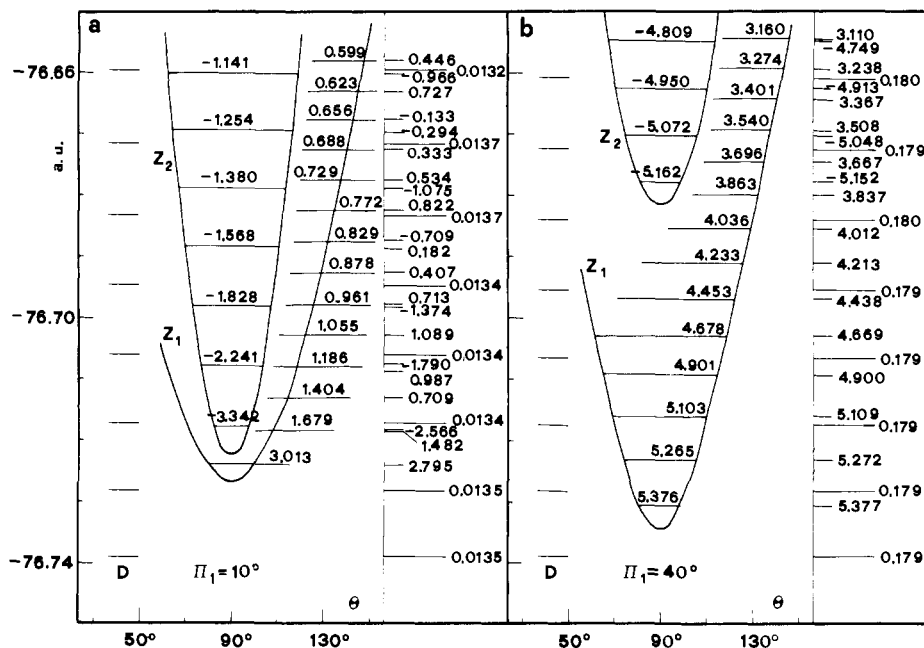


**Figure 5.** Vibrational energy levels of ethylene for the twisting coordinate, in the D,  $Z_1$ , and  $Z_2$  states, and average dipole moments (Born–Oppenheimer approximation). On the right, the energy levels and dipole moments, modified by the nonadiabatic coupling: a,  $\pi_1 = 10^\circ$ ; b,  $\pi_2 = 40^\circ$ .

is stabilized: the energy gap should increase. A calculation on twisted vinyl fluoride confirms this prediction, yielding  $\Delta E(Z_2 - Z_1) = 0.093$  au and a dipole moment of  $-5.0$  D (notice that a naive consideration based on the electronegativities would suggest the opposite dipole orientation). Also, let us consider the substitution of the  $H_3$  atom in the methyl group by a halogen atom, X; the a–c interaction will be weaker than in propene itself, because the c orbital is lower in energy and delocalized towards the X atom; the a–c\* interaction is reinforced for analogous reasons; altogether, we expect a decrease in the energy gap, and this is indeed the result of a calculation on the twisted 3-fluoropropene:  $\Delta E(Z_2 - Z_1) = 0.013$  au.

At the end of this decreasing series of  $\Delta E$  we could place the twisted butadiene, where the a orbital interacts with  $\pi$  and  $\pi^*$  orbitals delocalized on two other carbon atoms. Of course, the perturbative scheme is less suitable here than in the case of propene; a more adequate model, which corresponds to the reality of small CI calculations,<sup>8</sup> consists of considering the a orbital as a part of an allylic system; the  $a^2$  structure would place two electrons in the allylic nonbonding orbital, approximately degenerate to the b orbital of  $C_2$ . The conclusion is that in butadiene the energy difference between  $Z_1$  and  $Z_2$  is very small, as computed by other authors; indeed, the orientation of the dipole itself in the  $Z_1$  state depends on the method and the basis set.<sup>6,8</sup> This ambiguity disappears when either  $C_1$  or  $C_2$  are pyramidalized, leading to a  $Z_1$  surface with two minima as in ethylene and propene.<sup>6</sup>

### Vibronic States and Dynamical Calculations

The main purpose of this work is to clarify the roles and the interplay of sudden polarization and nonadiabatic coupling in the cis–trans isomerization of olefins. To this aim, we have performed a series of calculations regarding the pyramidalized ethylene (and propene) as a molecule made of two rigid fragments, which are only allowed to rotate one with respect to the other.

The first step is to expand in Fourier series all the functions of  $\theta$  relevant to the problem:  $U_K, \mu_{KL}, g_{KL}$ . The relative quadratures are performed with the aid of spline interpolation; up to 50 terms were included (60 terms for ethylene with  $\pi_1 = 10^\circ$ ). This facilitates the computation of all the necessary matrix elements.

Subsequently, the vibrational states are determined in the Born–Oppenheimer approximation; the moment of inertia of a  $-CH_2$  ( $I = 11\,000$  au) has been adopted for the twisting of propene and half of this value for ethylene. On the basis of the BO vibronic wave functions,  $\varphi_K(q, \theta)\chi_{K\mu}(\theta)$ , we compute the matrix elements

of the dipole operator and of the nonadiabatic coupling operator

$$h_{KL\mu\nu} = -\frac{1}{I} \left\langle \chi_{K\mu} \left| g_{KL}(\theta) \frac{\partial}{\partial \theta} + \frac{1}{2} t_{KL}(\theta) \right| \chi_{L\nu} \right\rangle \quad (1)$$

where

$$t_{KL}(\theta) = \left\langle \varphi_K \left| \frac{\partial^2}{\partial \theta^2} \right| \varphi_C \right\rangle = \sum_j g_{Kj} g_{jL} + \frac{\partial g_{KL}}{\partial \theta}$$

(for an analogous computational scheme with nonperiodic potentials (see ref 38)).

The molecular Hamiltonian matrix, including the nonadiabatic coupling, is then diagonalized to get the molecular eigenstates expanded in the basis of the BO states. At this point it is straightforward to compute the time evolution of an arbitrary wave function which could be put in the form of a linear combination of eigenstates.

The  $C_{2v}$  symmetry of the molecular problem (see above) is adequately exploited throughout the computational steps.

The whole calculation has been repeated for ethylene with  $\pi_1 = 10, 20$ , and  $40^\circ$  and for unpyramidalized propene.

Let us examine first the “static” results (Figure 5). The most interesting features concern the vibrational BO states of  $Z_1$  and  $Z_2$ . In the  $v = 0$  state we find the following ratios of the averaged dipole moment to its maximum value (at  $\theta = 90^\circ$ )

	$Z_1$	$Z_2$
ethylene, $\pi_1 = 10^\circ$	0.722	0.804
ethylene, $\pi_1 = 20^\circ$	0.934	0.952
ethylene, $\pi_1 = 40^\circ$	0.992	0.993
propene	0.986	0.988

We are thus far from the results of Orlandi et al., mimicking the case of *s-cis*, *s-trans* diallyl. In  $Z_2$  the average dipole is larger because the vibrational probability amplitude is more concentrated near  $\theta = 90^\circ$ . At higher vibrational quantum numbers the dipole decreases steadily in both states.

Figure 5 shows all these features, together with the effect of allowing for the nonadiabatic perturbation, at  $\pi_1 = 10^\circ$  and  $\pi_1 = 40^\circ$ . The  $g_{12}$  and  $g_{13}$  couplings are substantially ineffective in perturbing the vibrational states of the D state, even the highly excited ones which lie close in to energy to those of  $Z_1$  and  $Z_2$ ;

(38) R. Cimbrigaglia, M. Persico, and J. Tomasi, *Chem. Phys.*, **34**, 103 (1978).

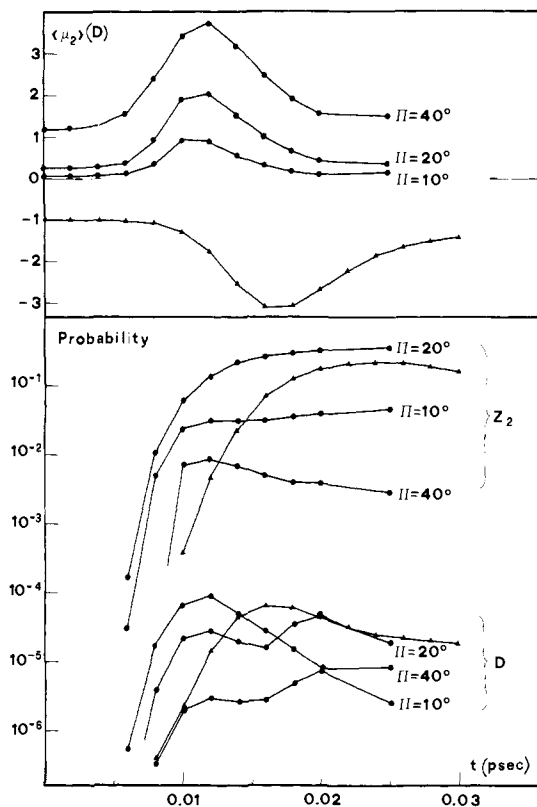


**Figure 6.** Time evolution calculations: at  $t = 0$ , Franck-Condon excitation to  $Z_1$ . Upper part: dipole moment in the  $Z_1$  state,  $\langle \mu_z \rangle = \langle \chi_2 | \mu_z | \chi_2 \rangle \langle \chi_2 | \chi_2 \rangle^{-1}$ . Lower part: transition probabilities to D and to  $Z_2$ ,  $\langle \chi_1 | \chi_1 \rangle$  and  $\langle \chi_3 | \chi_3 \rangle$ ; ▲ = propene; ● = ethylene at various pyramidalization angles.

in fact, the matrix elements of eq 1 are small in this case, because of the rapid oscillations in  $\chi_{1\mu}$ ; as commonly realized, this is the way through which the D -  $Z_1$  energy gap acts to hamper the decay from the excited state (see below).

The BO states pertaining to  $Z_1$  and  $Z_2$  are coupled between themselves to a larger extent, as can be guessed from the dipoles in the "molecular" eigenstates, reported in the right-hand sides of Figure 5a,b. The  $g_{23}$  coupling function, near the minimum in the  $Z_{1,2}$  energy curves  $U(\theta)$ , is larger at small (nonzero) pyramidalization angles; this behavior, together with the energy gap effect, makes the nonadiabatic perturbation more effective at  $\pi_1 = 10^\circ$  and  $20^\circ$  than at  $\pi_1 = 40^\circ$ . In any case, however, the lowest vibrational state(s) in  $Z_1$  keeps its strongly polar character.

The dynamical calculations have been performed mainly in order to find the order of magnitude of the  $Z_1 \rightarrow D$  transition probability during an oscillation in the excited state. At  $t = 0$  the system is represented as a superposition of vibrational eigenfunctions of the  $Z_1$  excited state, with coefficients proportional to the dipolar transition matrix elements to the BO ground state (Franck-Condon excitation). At all the following times the molecular wave function can be written as a superposition of products of electronic and vibrational factors

$$\Psi(q, \theta, t) = \sum_K \varphi_K(q, \theta) \chi_K(\theta, t) \quad (2)$$

In the upper part of Figure 6 we show the time dependent dipole moment in the  $Z_1$  state

$$\langle \mu_z \rangle = \langle \varphi_2 \chi_2 | \mu_z | \varphi_2 \chi_2 \rangle \langle \varphi_2 \chi_2 | \varphi_2 \chi_2 \rangle^{-1} = \langle \chi_2 | \mu_z | \chi_2 \rangle \langle \chi_2 | \chi_2 \rangle^{-1} \quad (3)$$

$\langle \mu_z \rangle$  could be said to "monitor" the evolution of the wavepacket: it is small at the beginning, it goes through a maximum at the first passage near  $\theta = 90^\circ$ , and then it decreases again. The

behavior of the total dipole,  $\langle \mu \rangle = \langle \Psi | \mu_z | \Psi \rangle$ , is similar, but its maximum value is smaller, due to the negative contribution of the  $Z_2$  state; altogether, this feature illustrates the reluctance of the electronic part of the wave function to change character and polarity too suddenly.

In the lower part of Figure 6 we show the probabilities of finding the system in the D and  $Z_2$  states, respectively  $\langle \chi_1 | \chi_1 \rangle$  and  $\langle \chi_3 | \chi_3 \rangle$ . The transition probability to the ground state never exceeds  $10^{-4}$  during the oscillation in  $Z_1$ , which makes a decay time of about  $10^{-9}$ – $10^{-10}$  s. The  $Z_2$  state, on the contrary, becomes rapidly populated. In any case, the nonadiabatic behavior is restricted to the region near  $\theta = 90^\circ$ , where the coupling is larger and the energy gaps smaller than elsewhere.

If the initial excitation leads to  $Z_2$  instead of  $Z_1$ , the subsequent time evolution is qualitatively similar.

### Conclusions

This work on the whole, and especially the quantum dynamical calculations, has a paradigmatic value rather than claiming to give quantitative answers to the problems raised. A more rigorous treatment of the coupling of different internal coordinates (first of all, twisting and pyramidalization) and of the excitation process, together with accurate electronic calculations, is the condition for a realistic description of the cis-trans photoisomerization in olefins.

Some important conclusions can be drawn from the present investigation, together with the preceding ones of other authors. (a) The excited, twisted, olefins can exist in highly polar states, not only electronic states at some particular geometry but also Born-Oppenheimer vibronic states; as brought out by Orlandi et al.,<sup>24</sup> a very small perturbation of a basically homosymmetric diradical could remain nearly without consequences at a molecular level (the case of *s-cis*, *s-trans* diallyl) should be regarded as a limiting situation); however, both a moderate pyramidalization, which is energetically favored in  $Z_1$ , and an unsymmetrical alkyl substitution play the role of strong perturbations in this context. (b) The nonadiabatic coupling between  $Z_1$  and  $Z_2$  does not destroy the polar character of the lowest ionic vibronic states. (c) The same coupling mixes the higher vibrational states of  $Z_1$  with those of  $Z_2$  and probably characterizes the dynamical behavior of an excited olefin in the very short time range ( $10^{-14}$ – $10^{-12}$  s); as a consequence, the interaction of the  $Z_1$  and  $Z_2$  states is relevant in the interpretation of the UV spectrum. (d) The nonadiabatic transition probability from  $Z_1$  to the ground state during a single twisting oscillation is much smaller than unity; hence, in setting up a model of the cis-trans photoisomerization, it seems acceptable to separate in the time scale the process of thermal equilibration, with relaxation to the twisted and pyramidalized geometry, and the subsequent radiationless decay.

As shown by the example of propene, the pyramidalized ethylene mimics very well the behavior of substituted monoolefins; the conjugated polyenes could exhibit other features, also concerning the nonadiabatic coupling, due to the presence of low-lying excited states of different nature.

**Acknowledgment.** The idea of this investigation was born in occasion of the C.E.C.A.M. workshop "The Sudden Polarization Effect" (Orsay, France, June 25–July 21, 1979); thanks are due to the organizer, L. Salem, to the director of the Centre, C. Moser, to all the participants, and in particular to V. Bonačić-Koutecký, B. Lévy, G. Orlandi, and A. Warshel for very helpful discussions and for communicating the results of their work prior to publication to me.

I also thank J. Tomasi and R. Cimraglia for helping me at each stage of this work and for reading and commenting upon the manuscript.

The necessary financial support was supplied by a grant of the Ministero della Pubblica Istruzione (No. 78-8598) and by the Italian C.N.R., through its Istituto di Chimica Quantistica ed Energetica Molecolare.